III-4

Surface, Interface and Thin Films

BL6U

The Photoelectron Momentum Microscope

F. Matsui[1], S. Makita[1], H. Matsuda[1], T. Yano[1], E. Nakamura[1], K. Tanaka[1,2], T. Ohigashi[1,2],
H. Horigome[1], S. Ideta[1,2], Y. Hasegawa[2], S. Suga[3] and S. Kera[1,2]
[1]*UVSOR Synchrotron Facility, Institute for Molecular Science, Okazaki 444-8585, Japan*
[2]*The Graduate University for Advanced Studies, SOKENDAI, Okazaki 444-8585, Japan*
[3]*The Institute of Scientific and Industrial Research, Osaka University, Ibaraki 567-0047, Japan*

The importance of characterizing microstructure electronic properties cannot be overemphasized. The demand for photoelectron micro-spectroscopy and spectro-microscopy is growing rapidly. Photoelectron spectroscopy resolved in three-dimensional momentum space with a microscopic field of view is realized by combining a so-called Momentum Microscope with a soft X-ray synchrotron radiation source. This method opens the door to direct observation of the Fermi surface of µm-sized crystals, which was difficult with conventional ARPES-type hemispherical analyzers. A new experimental station for Momentum Microscopy has been built at BL6U, an undulator-based soft X-ray beamline. In fact, this successful combination of a single HDA-type Momentum Microscope at the synchrotron facility is the first case in the world. As shown in Fig.1, the system consists of a photoemission electron microscope (PEEM) lens, a hemispherical deflection analyzer (HDA) for imaging-type energy filter, and a 2D detector with a CMOS camera. This experimental station specializes in characterizing the electronic structure of surface atomic sites, thin films, molecular adsorbates, and bulk crystals.

The details of the specification evaluation result are described elsewhere [1]. In brief, the energy resolution of the analyzer was estimated to be 22.74 meV at pass energy of 20 eV. The spatial resolution in the microscopy mode was evaluated to be about 50 nm. The momentum resolution of 0.012 Å^{-1} has been achieved. The position of sample stage facing to the analyzer is precisely controlled by a hexapod. Samples can be cooled down to 10 K and heated up to 400 K.

Figure 2 shows the optical and PEEM images of a piece of micro channel plate (MCP) fragment. The pore size was 10 µm and the interval of each pore was 11.6 µm. The top surface of the MCP is clearly imaged, despite the nearby deep holes and useful for the lateral length calibration. It is interesting to note that excited photoelectrons are detected from one side of the hole wall. Figure 3 shows the preliminary results of valence band photoelectron 2D angular patterns excited by He lamp and synchrotron radiation. The six bright spots correspond to the π band at the vicinity of Dirac cone. The center double ring structure originates from the substrate Ru 4*d* band.

We greatly acknowledge Dr. Markus Breusing, Dr. Marko Wietstruk, and Dr. Mirko Weidner (SPECS) and Dr. Dai Yamaguchi (Tokyo Instruments Inc.) for their contribution in the construction of the BL6U Momentum Microscope experimental station.

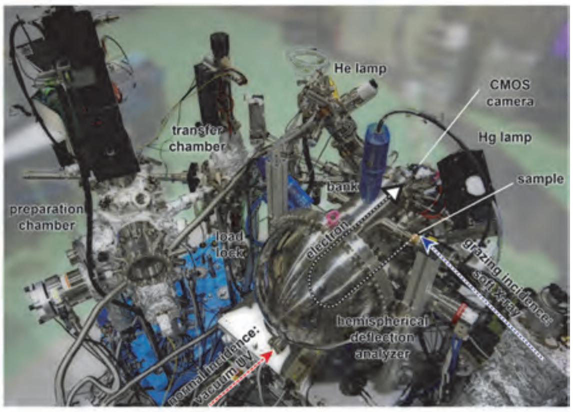

Fig. 1. Photograph of the Momentum Microscopy station at BL6U.

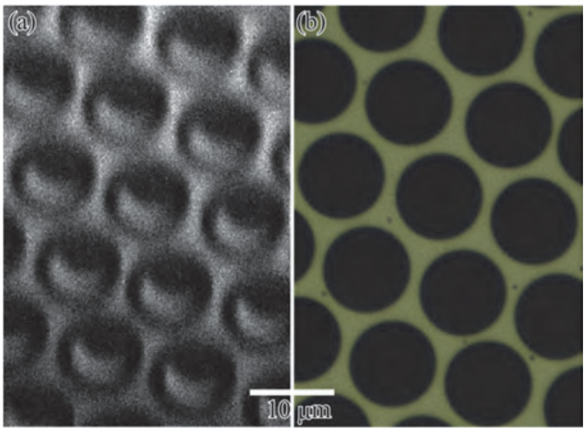

Fig. 2. (a) Optical photograph and (b) PEEM image of a honeycomb pattern.

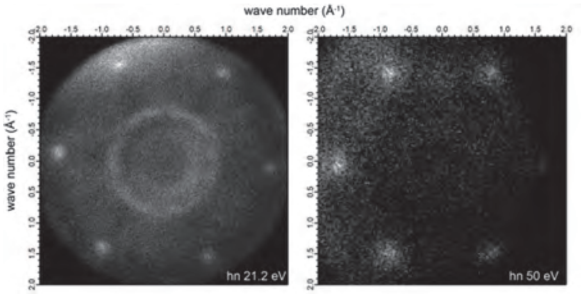

Fig. 3. Photoelectron angular distribution of valence band from graphene grown on the Ru(111) surface excited by (a) He lamp and (b) synchrotron radiation.

[1] F. Matsui *et al.*, Jpn. J. Appl. Phys. **59** (2020) 067001.

BL2A

NEXAFS Spectroscopy of Magnesium Oxide Powder

E. Kobayashi[1], K. K. Okudaira[2], T. Kikuchi[2], M. Imamura[3], K. K. Bando[3], S. Yoshioka[4]
and O. Takahashi[5]
[1]Kyushu Synchrotron Light Research Center, Tosu 841-0005, Japan
[2]Chiba University, Chiba 263-8522, Japan
[3]National Institute of Advanced Industrial Science and Technology, Tsukuba 305-8565, Japan
[4]Graduate School of Engineering, Kyushu University, Fukuoka 819-0395 Japan
[5]Graduate School of Science, Hiroshima University, Higashi-Hiroshima, 739-8526, Japan

Magnesium oxide (MgO) has been widely used as catalytic, optical and electrical applications [1]. In recent years, the performance of not only organic photovoltaics but also perovskite solar cells has been successfully improved by employing MgO nanolayers as electrodes [2,3].

In order to further improve the characteristics of such solar cells, it is necessary to understand the surface and bulk electronic states. Near-edge X-ray absorption fine structure (NEXAFS) spectroscopy is a powerful tool for investigating the electronic structures of materials. The NEXAFS spectra can be obtained by electron yield (EY) mode or fluorescence yield (FY) mode. The former is sensitive to the surface and the latter is sensitive to the bulk.

In this study, we measured Mg *K*-edge NEXAFS spectra of MgO using both total electron yield (TEY) and partial fluorescence yield (PFY) modes in order to investigate the change in surface and bulk states with particle size.

Two MgO powders with different particle size were prepared. One is the size of 50 nm or less (MgO_A). The other is 50 nm average (MgO_B). NEXAFS spectra of the MgO powders were measured at the beamline 2A of the UVSOR in the Institute of Molecular Science. For TEY, the drain current from the sample was measured. For PFY fluorescence X-rays were collected using an energy dispersible silicon drift detector (SDD). All experiments were performed at room temperature.

Figure 1 shows the Mg *K*-edge NEXAFS spectra of MgO powder obtained from TEY and PFY. In the spectrum measured in the TFY mode, the spectra of MgO_A and MgO_B showed almost the same shape. Their spectra were different from the $Mg(OH)_2$ spectra measured as a reference. On the other hand, in the spectrum measured in the TEY mode, the spectra of MgO_A and MgO_B were different. The spectrum of MgO_A was almost similar to the spectrum of $Mg(OH)_2$ measured as a reference. These results indicate that the bulk of MgO_A is MgO, but the surface is $Mg(OH)_2$. Since MgO_A has a smaller particle size than MgO_B, the surface has high activity. Therefore, $Mg(OH)_2$ formed on the surface of MgO_A with water in the atmosphere.

As a next step we will clarify the electronic structure of the interface between organic semiconductors and MgO nanolayers.

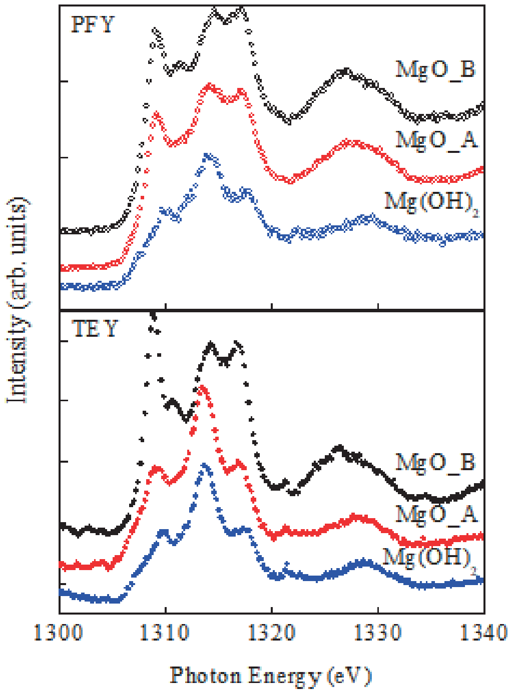

Fig. 1. Mg *K*-edge NEXAFS spectra of MgO powder.

[1] E. A. Colbourn, Surf. Sci. Rep.**15** (1992) 281.
[2]H. J. Bolink, H. Brine, E. Coronado and M. Sessolo, J. Mater. Chem. **20** (2010) 4047.
[3] J. Ma, G. Yang, M. Qin, X. Zheng, H. Lei, C. Chen, Z. Chen, Y. Guo, H. Han, X. Zhao and G. Fang, Adv. Sci. **4** (2017) 1700031.

BL2B

Electronic Structure of ZnO Nanoparticles Deposited on ITO

K. K. Okudaira and T. Kikuchi
Association of Graduate Schools of Science and Technology, Chiba University, Chiba 263-8522, Japan

Organic photovoltaic cells (OPV) have been attracting interest concerning both fundamental research and practical application for low-cost, large-area, lightweight and flexible devices. In recent years, various solution-processed bulk-heterojunction photovoltaic devices have been reported using p-type conjugated polymers, either in combination with n-type inorganic semiconductor nanoparticles. These hybrid polymers: inorganic - nanoparticle bulk heterojunctions can take advantage of the beneficial properties of both types of materials: solution processing of polymer semiconductors and high electron mobility of inorganic semiconductors.

The characteristics of OPV such as efficiency and filling factor are considered to be dependence on the electronic structure of not only organic semiconductor but also n-type inorganic semiconductor nanoparticles.

In this work we deposited ZnO nanoparticles (NPs) thin films on ITO and clarify the electronic structure of ZnO NPs using hν-dependence of ultraviolet photoelectron spectroscopy (UPS) measurements.

We synthesized ZnO NPs with different particle size. The size of nanoparticles synthesized by ref [1] is about 5 nm. On the other hand, the size of ZnO nanoparticle synthesized by ref [2] is about 80 nm, which is ten times larger than that synthesized by the first methods. Here after we refer the ZnO nanoparticles by the first method and the second method to ZnOs and ZnO200, respectively. UPS measurements were performed at the beam line BL2B of the UVSOR storage ring at the Institute for Molecular Science. UPS were measured with the photon energy (hν) of 28 eV and 40 eV. The ZnO NP thin films were prepared by spin-cast on ITO. The ZnO NP thin films were annealed at 120 °C.

We observed hν)dependence of UPS of ZnO NPs with different particle size (ZnOs and ZnO200) on ITO (Fig. 1). In the UPS three broad peaks appear about Eb (binding energy) of about 5 eV, 7.5 eV, and 10 eV. These peaks around 5 eV and 7.5 eV are assigned to the states which are hybridized Zn 4s and O 2p orbitals. By considering the photoionization cross section of O 2p and Zn 4s of hν of 28 eV and 40 eV, the peak at lower binding energy and that at higher binding energy is made of mainly by O 2p and Zn-4s, respectively. The peak at Eb of about 10 eV is the emission of the Zn 3d band. These assignments are good agreement with ref [3]. In Fig. 2 the annealing processes do not affect the UPS of ZnOs as well as ZnO200. On the other hand, the relative peak intensity of the peak about 10 eV to that about 5 eV of ZnOs is larger than that of ZnO200. It is considered that the two synthetic methods provide the different surface structures such as the introduction of hydroxyl group.

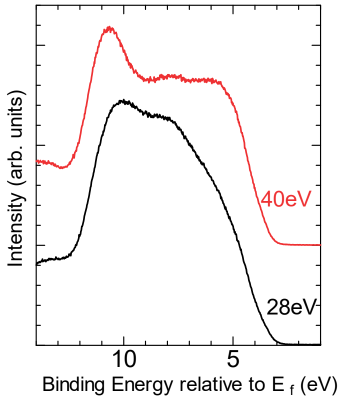

Fig. 1 UPS of ZnO NPs (ZnOs) at hν of 28 eV and 40 eV.

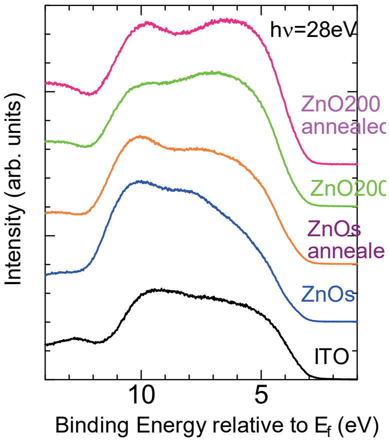

Fig. 2 UPS of ZnO nanoparticles (ZnOs and ZnO200) at hν of 28 eV.

[1] N. M. Shamhari, B. S. Wee, S.F. Chin and K. Y. Kok, Acta Chim. Slov. **65** (2018) 578.
[2] H. Du, F. Yuan, S. Huang, J. Li and Y. Zhu, Chem. Lett. **33** (2004) 770.
[3] W. Ranke, Solid State Commun. **19** (1976) 685.

BL3U

Cobalt Oxide Catalyst in Carbonate Aqueous Solution Studied by Operando C K-edge XAFS Measurement

T. Moriyama[1], M. Nagasaka[2], H. Yuzawa[2] and M. Yoshida[1,3]
[1]*Faculty of Engineering, Yamaguchi University, Ube 755-8611, Japan*
[2]*Institute for Molecular Science, Okazaki 444-8585, Japan*
[3]*Blue energy center for SGE technology (BEST), Yamaguchi University, Ube 755-8611, Japan*

Electrochemical water splitting with renewable energies is attracting attention as a sustainable hydrogen production technique. In the electrolysis of water, overvoltage of the oxygen evolution reaction (OER) is a problem, and the development of a highly active OER electrocatalyst is strongly required. In this situation, a nickel carbonate (Ni-C_i) was reported recently as an OER catalyst with high activity [1]. Meanwhile, we revealed the function of similar cobalt OER catalysts by operando X-ray absorption fine structure (XAFS) observation [2]. Therefore, we attempted to clarify the structure and reaction mechanism of the Ni-C_i catalyst by performing operando soft X-ray XAFS measurements.

A electrochemical cell was equipped with a Pt counter electrode and an Ag/AgCl reference electrode for all electrochemical experiments. The Ni-C_i thin films were electrodeposited on Au thin film in potassium carbonate aqueous solution containing $Ni(NO_3)_2$ at 1.7 V vs. RHE. The operando O *K*-edge and C *K*-edge XAFS spectra for Ni-C_i were taken under electrochemical control with transmission mode at BL3U in the UVSOR Synchrotron, according to the previous works [3].

First, we checked the electrochemical OER activity for Ni-C_i catalyst and confirmed that the catalyst can decompose water efficiently. The surface states and chemical composition were also measured by SEM, EDX, stylus profilometer.

Next, operando O-*K* edge XAFS spectra were measured for Ni-C_i catalyst under electrochemical condition. In this spectra, a peak coincided with that of γ-NiOOH of the reference sample was observed at around 528.6 eV, indicating that the Ni-C_i catalyst changed its structure to γ-NiOOH during the OER process.

Finally, operando C-*K* edge XAFS measurements were performed, as shown in Figure 1. At the non-active potential of 1.2 V, a peak was observed at around 290.3 eV near the peak position of carbonate ion, suggesting that the carbonate ion was adsorbed on the Ni-C_i catalyst. Furthermore, when the electrode potential changed from 1.2 V to 1.7 V, the carbonate peak shifted to a higher energy side. This phenomenon is presumed to be due to the direct adsorption of carbonate ion on the γ-NiOOH as active species. Thus, we suggest that the adsorption of carbonate ion is likely to contribute the stabilization of γ-NiOOH and that the Ni-C_i catalyst has high OER activity by the existence of γ-NiOOH with highly active reaction sites.

In conclusion, we revealed the function of Ni-C_i electrocatalyst by operando O *K*-edge and C *K*-edge XAFS measurements. It was exhibited that the carbonate species was adsorbed on the γ-NiOOH structure to stabilize the active reaction sites, and the interface of γ-NiOOH and adsorbed carbonate ion is likely to function as efficient OER site.

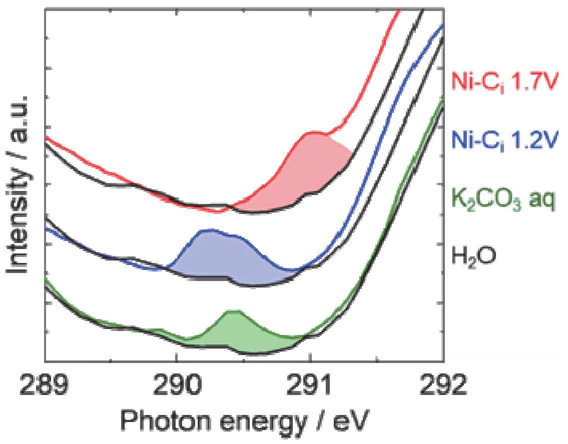

Fig. 1. Operando C *K*-edge XAFS spectra for Ni-C_i at 1.2 V (non-active state) and 1.7 V (active state) vs. RHE, together with the saturated K_2CO_3 aqueous solution.

[1] (a) M. Ma, Y. Liu, X. Ma, R. Ge, F. Qu, Z. Liu, G. Du, A. M. Asiri, Y. Yao and X. Sun, Sustainable Energy Fuels **1** (2017) 1287.
(b) K. S. Joya, Y. F. Joya and H. J. M. de Groot, Advanced Energy Materials **4** (2014) 1301929.
[2] K. Yamada, T. Hiue, T. Ina, K. Wang, H. Kondoh, Y. Sakata, Y. L. Lee, T. Kawai and M. Yoshida, Anal. Sci. **36** (2020) 35.
[3] (a) M. Nagasaka, H. Yuzawa, T. Horigome and N. Kosugi, Rev. Sci. Instrum. **85** (2014) 104105.
(b) M. Yoshida, Y. Mitsutomi, T. Mineo, M. Nagasaka, H. Yuzawa, N. Kosugi and H. Kondoh, J. Phys. Chem. C **119** (2015) 19279.

BL3U

In Situ XAFS Study of Pt Subnanoparticles on the Oxygen Reduction Reaction

A. Kuzume[1], M. Nagasaka[2] and K. Yamamoto[1]
[1]*JST-ERATO, Yamamoto Atom Hybrid Project, Institute of Innovative Research, Tokyo Institute of Technology, Yokohama 226-8503 Japan*
[2]*Institute for Molecular Science, Okazaki 444-8585, Japan*

Subnanoparticles (SNPs) is a new-generation material with a particle diameter of about 1 nm, composing only several tens of atoms. Due to its small number of constituent atoms (atomicity), it exhibits unique properties not commonly found in bulk and nanomaterials. However, it was difficult to understand the detailed characteristics and chemical activity of SNPs because of its difficulty in synthesis and analysis.

In our laboratory, we have established a liquid-phase SNPs synthetic method using a dendritic polymer called 4th generation Tetraphenylmethane-core, phenylazomethine dendrimer (TPM-DPA-G4) as a template macromolecule, which can control the atomicity precisely [1-3]. With this technique, scalable synthesis of SNPs is possible, and thus detailed analyses of physical, chemical and electric properties, as well as chemical activities, of SNPs is expected [4].

Pt SNPs have been synthesized using the method described above and were found to exhibit unique catalytic activities on electrochemical oxygen reduction reaction (ORR), which is the key cathodic reaction for the fuel cell development. Pt SNPs were found to exhibit discrete catalytic activity on ORR, depending on the atomicity [5-7]. To evaluate its specificity, it is necessary to monitor changes in the electron state of SNPs during the electrochemical reaction. In this study, in situ XAFS measurements of Pt SNPs on O K-edge were performed at BL3U in UVSOR facility to elucidate precise atomicity-dependent ORR activity by monitoring the state of Pt oxide on the surface of SNPs under electrochemical condition.

The home-made in situ XAFS cell with the electrochemical setup was used [8], where Pt SNPs were cast on a carbon-film modified on the silicon nitride substrate (10 mm x 10 mm). A Pt wire and Ag/AgCl electrode were used as a counter and reference electrode. Air-saturated 0.1M $HClO_4$ solution (prepared with MERCK Suprapur $HClO_4$ and ultrapure water from the Milli-Q system) were constantly supplied during the in situ measurement by the peristaltic pump.

Figure 1 shows the potential dependent in situ XAFS spectra of O K-edge on Pt_{12} SNPs. It was not easy to identify the potential dependence in the series of spectra due to significantly low signal intensity of O species adsorbed on Pt surface. Difficulty in the characterization of SNPs is mainly originated from their size. In general, the signal intensity of SNPs in the vibration spectroscopic study, such as infrared and Raman spectroscopy, is far below the detection limit with the conventional technique and requires improvement in sensitivity to detect SNPs [9]. To increase the signal intensity of XAFS spectra, one needs to increase the amount/surface coverage of Pt SNPs in our electrochemical XAFS setup. However, due to the principle of the measurement, one needs to keep the thickness of the sample as low as possible to increase the transmission rate. This trade-off situation makes it difficult to detect O species on Pt SNPs.

In conclusion, our preliminary results indicated that the transmission detection configuration needs to be changed to the fluorescence mode, where one can simply increase the amount of Pt SNPs to improve the detection sensitivity.

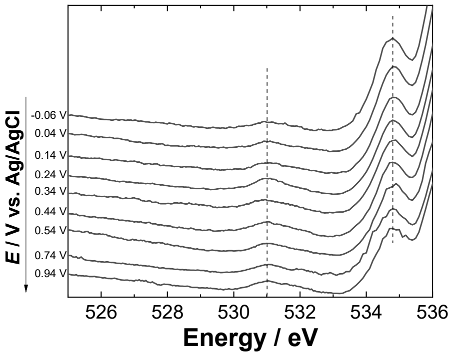

Fig. 1. Potential dependent in situ O K-edge XAFS spectra of Pt_{12} SNPs in 0.1M $HClO_4$ versus Ag/AgCl.

[1] A. Kimoto, K. Masachika, J.S. Cho, M. Higuchi and K. Yamaomto, Org. Lett. **6** (2004) 1179.
[2] O. Enoki, H. Katoh and K. Yamamoto, Org. Lett. **8** (2006) 569.
[3] K. Yamamoto, M. Higuchi, S. Shiki, M. Tsuruta and H. Chiba, Nature **415** (2002) 509.
[4] K. Yamamoto and T. Imaoka, Acc. Chem. Res. **47** (2014) 1127.
[5] K. Yamamoto, T. Imaoka, W.J. Chun, O. Enoki, H. Katoh, M. Takenaga and A. Sonoi, Nat. Chem. **1** (2009) 397.
[6] T. Imaoka, H. Kitazawa, W.J. Chun and K. Yamamoto, Angew. Chem. Int. Ed. **54** (2015) 9810.
[7] T. Imaoka, Y. Akanuma, N. Haruta, S. Tsuchiya, K. Ishihara, T. Okayasu, W.J. Chun, M. Takahashi and K .Yamamoto, Nat. Commun. **8** (2017) 688.
[8] M. Yoshida, Y. Mitsutomi, T. Mineo, M. Nagasaka, H. Yuzawa, N. Kosugi and H. Kondoh, J. Phys. Chem. C **119** (2015) 19279.
[9] A. Kuzume, M. Ozawa, Y. Tang, Y. Yamada, N. Haruta and K. Yamamoto, Sci. Adv. **5** (2019) eaax6455.

BL3B

Clarify of Formation Process and Optical Properties Evaluation of Ultra-Violet Emitting Zinc Aluminate Phosphor Thin Films

H. Kominami[1], M. Arimura[1], K. Imagawa[1], K.Warita[2], S. Nishibori[2], M. Endo[2],
T. Kawashima[2], N. Sonoda[2], S. Kodama[3] and S. Kurosawa[3,4]
[1]*Graduate School of Integrated Science and Technology, Shizuoka University, Hamamatsu 432-8651, Japan*
[2]*Faculty of Engineering, Shizuoka University, Hamamatsu 432-8651, Japan*
[3]*New Industry Creation Hatchery Center (NICHe), Tohoku University, Sendai 980-8579, Japan*
[4]*Faculty of science, Yamagata University, Yamagata 990-8560, Japan*

The UV light is used for various applications depending on the wavelength as well as the sterilization described above. The lights of 200-280 nm (UV-C) region as for the sterilization, 280-320 nm (UV-B) region as the treatment of the skin disease, 320-400 nm (UV-A) region as application of purification of water and air, and photocatalysts. Recently, from the viewpoint of consideration to the environment, the mercury free UV emission devices have been demanded for the application of catalyst and medical situations. In our previous work, it was clarified that $ZnAl_2O_4$ phosphor was suitable for the UV field emission lamp because of its stability and luminescent property. It shows strong UV emission peaked around 250 nm which suitable for sterilization.

Conventionally, powder samples have been prepared and evaluated, but it was difficult to analyze transmittance and refractive index due to the influences of surface scattering, so it would be possible to evaluate these basic physical properties by preparing thin film samples. In this research, ZnO films were deposited on sapphire substrates by sputtering and $ZnAl_2O_4$ thin films were prepared by thermal diffusion. These films were evaluated the orientation and crystallinity. Quality of thin films were evaluated by relationships between UV emission intensity and penetration depth of electron beam, and also the distribution of Zn and Al was studied using cross sectional FE-EPMA to analyze the emitting layer.

Figure 1 shows the XRD patterns of thin films prepared on a-plane sapphire substrate. Before annealing, any diffraction peaks of ZnAl2O4 were not observed, however ZnO (002) peak was confirmed near 34°. After annealing, diffraction peak of $ZnAl_2O_4$ (333) appeared, and selective growth was confirmed. FWHM of diffraction peaks of $ZnAl_2O_4$ (333) decrease according to inarticulate interface of each layer, the multilayer film containing constituent elements was formed by sputtering on quartz substrate, and tried to prepare the $ZnAl_2O_4$ thin film by thermal diffusion.

Figure 2 shows PL spectra of $ZnAl_2O_4$ thin film annealed for 15 hours excited by VUV. From the spectra, ZnO emission around 380 nm and 520 nm (caused from exiton and oxygen vacancy, respectively) were not observed. It indicates that ZnO layer were diffused to substrate completely and re-evaporated. It is thought that the 50 hours or more thermal annealing is necessary for obtain the good quality $ZnAl_2O_4$ thin film preparation.

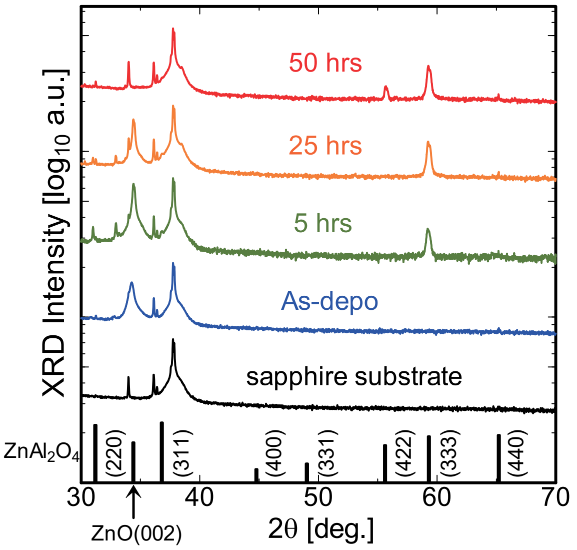

Fig. 1 XRD patterns of films on a-plane sapphire substrate before and after annealing for several hours.

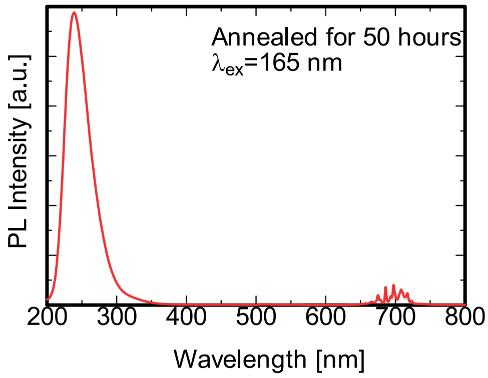

Fig. 2 PL spectra of $ZnAl_2O_4$ thin film.

BL4U

Microscopic Electronic Structure of Vanadium Nitride/Oxide Supercapacitors

H. W. Shiu[1], L. C. Yu[1], Y. L. Lai[1], T. Ohigashi[2], Y.-G. Lin[1] and Y. J. Hsu[1]
[1]National Synchrotron Radiation Research Center, Hsinchu 300, Taiwan
[2]Institute for Molecular Science, Okazaki 444-8585, Japan

How to provide an environmentally friendly energy system with high performance and low cost has become an important issue due to the rapid growth of electric vehicles and portable electronic devices. Supercapacitors (SCs), also called electrochemical capacitors, have attracted a lot of attentions due to their specific advantages of fast power release and long cycle-life [1]. However, the existing commercialized carbon electrode has the bad traits of low specific capacitance. Accordantly, the main research targets of SCs mainly focused on the development of pseudo-capacitive electrode materials. Transition metal oxide, nitride, sulfide and conducting polymers have been experimentally demonstrated as a promising electrode material for the next generation SCs [2].

Recently, the earth-abundant and inexpensive materials i.e. vanadium oxides (VOx), have been intensely investigated as cathode materials for SCs. The multiple stable oxidation states and layered structure enable it to have a higher storage capability. A similar material named Vanadium nitride (VN) holds great promise as an advanced electrode for asymmetric super capacitors due to its large specific capacitance (1340 F/g) and superb electrical conductivity (106/Ωm). In our previous studies we also observed that the capacitance retention is enhanced as high as 90% at high current density. Only 5.9% decay was observed at 1000 cycles.

In order to understand the mechanism of the enhancement of the specific capacitance and the capacitance retention, we synthesized a set of VON and VN through the electrochemical deposition in an electrolyte solution containing Na_2SO_4 and NH_4VO_3 for 6 hours and post-treatment at 500 to 700 degree Celsius under NH_3 condition. A systematically study for the set of materials was made by scanning transmission X-ray microscopy (STXM) and Near-edge X-ray absorption fine structure (NEXAFS) at UVSOR BL4U and TLS 09A2, respectively.

Figure 1 shows the XAS spectra of VON and VN powders transferred onto Si substrate measured at TLS BL 09A2 with the photon beamsize of 100 μm. The “average” spectrum of VN has no oxygen feature and the characteristic peaks of V L-edge shifted to lower photon energy which clearly indicated that the valence state is altered to the lower oxidation state.

To investigate the chemical distribution of the VON powders, multiple sets of STXM images at different photon energy have been measured. The results display the STXM element mapping as shown in Fig. 2 (a). All of the VON samples exhibit nano-rod structure with the dimension of ~ 150 nm in diameter and ~ 1 μm in length.

Figure 2 (b) shows the XAS spectra near the V L-edge and O K-edge extracted from Fig. 2 (a). The two major peaks at ~ 518 and 525 eV are the V L_{III} and L_{II} peaks, respectively. Different from the broadened peak of V L_{II}-edge, the three considerable peaks were observed at V L_{III}-edge correspond to the transition from V $2p_{3/2}$ to t_{2g} (π^*), t_{2g} (d^*) and e_g (σ^*), respectively. The two clear features between 527 to 534 eV are the transition from O 1s to the hybridized O 2p/V 3d, i.e. t_{2g} and e_g orbitals. Significant intensity changes between those two peaks (O K-edge, $t2_g$ and e_g) may result from the ununiform valence state of N-V-O bound and polarization effect [3]. Further experiments are needed to confirm this observation.

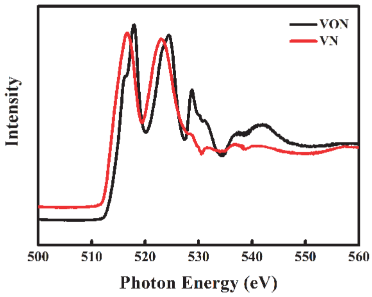

Fig. 1. V L-edges and O K-edge XAS spectra of VON and VN measured at Taiwan Light Source (TLS).

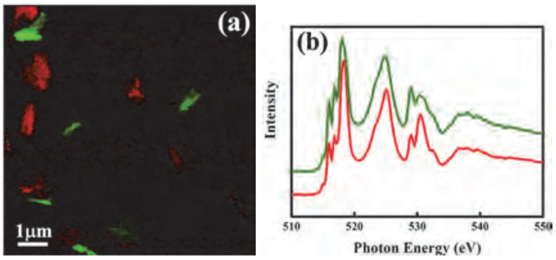

Fig. 2 (a) Color-coded composite mapping of VON powder identified by the O K-edge spectra (e_g/t_{2g}) and (b) the corresponding micro-spectra of red and green areas.

[1]Y. Yang, G. Ruan, C. Xiang, G. Wang and J. M. Tour, J. Am. Chem. Soc. **136** (2014) 6187.
[2] H. Pang, C. Wei, X. Li, G. Li, Y. Ma, S. Li, J. Chen and J. Zhang, Sci. Rep. **4** (2014) 3577.
[3] D. Maganas, M. Roemelt, M. Hävecker, A. Trunschke, A. Knop-Gericke, R. Schlögl and F. Neese, Phys. Chem. Chem. Phys. **15** (2013) 7260.

BL4B

Absorption Spectra of Amorphous Chalcogenide Thin Films in the Vacuum Ultraviolet Region

K. Hayashi
Department of Electrical, Electronic and Computer Engineering, Gifu University, Gifu 501-1193, Japan

Amorphous chalcogenide semiconductor materials are very photosensitive materials and show a variety of photo-induced phenomena. Therefore, these materials are expected as materials for optoelectronic devices. A lot of work have been done on the photo-induced phenomena of these amorphous semiconductor materials and various mechanisms have been proposed for these photo-induced phenomena [1-3]. However, the details of the mechanisms are still unknown. For device applications, it is necessary to sufficiently understand the fundamental properties of these materials. These phenomena have been studied by exciting outer core electrons by irradiating light with the energy corresponding to the optical bandgap or sub-bandgap. The interest has been attracted for the change of the optical properties in the energy region of the visible light. We are interesting for the changes of the optical properties in the higher energy region. To our knowledge, little attention has been given to photo-induced changes at the vacuum ultra-violet (VUV) absorption spectrum. In this report, we report the VUV absorption spectra of as-deposited evaporated amorphous Se and As_2Se_3 thin films.

Samples used for the VUV absorption spectrum were amorphous Se and As_2Se_3 thin films prepared onto aluminum thin films by conventional evaporation technique. Typical thickness of the amorphous film and the aluminum film were around 200 nm and 100 nm, respectively. The aluminum film of the thickness of 200 nm was also used in order to eliminate the higher order light from the monochromator in the VUV region. The measurements were carried out at room temperature at the BL4B beam line of the UVSOR facility of the Institute for Molecular Science. And the spectrum was measured by using the silicon photodiode as a detector. A pinhole of 1.5 mm in a diameter was inserted between the monochromator and sample to remove stray light. The intensity of the VUV light was monitored by measuring the total photoelectron yield of a gold mesh. The positions of the core levels for the samples were calibrated by referencing to the 2p core level absorption peak of the aluminum film.

Figure 1 shows the VUV absorption spectra of as-deposited amorphous Se and As_2Se_3 thin films at room temperature. The structure observed in this energy region from 40 to 55 eV is due to the transitions from the As 3d core level. On the other hand, the structure observed in this energy region from 55 to 70 eV is due to the transitions from the Se 3d core level. As shown in the figure, each spectrum is very broad and multiple shoulders are observed. The structure in the spectrum of amorphous As_2Se_3 is good agreement with previous report [4]. On the other hand, the spectrum shape of the main peak of amorphous Se is slightly different from the previous report. It can be attributed to the spin-orbit splitting of the 3d core level of each atom as observed by XPS. It is not clear about the origin of broad spectra and shoulders. I think that these origins are related to the local structures of the amorphous network. The detailed experiments and analysis will be done in the next step.

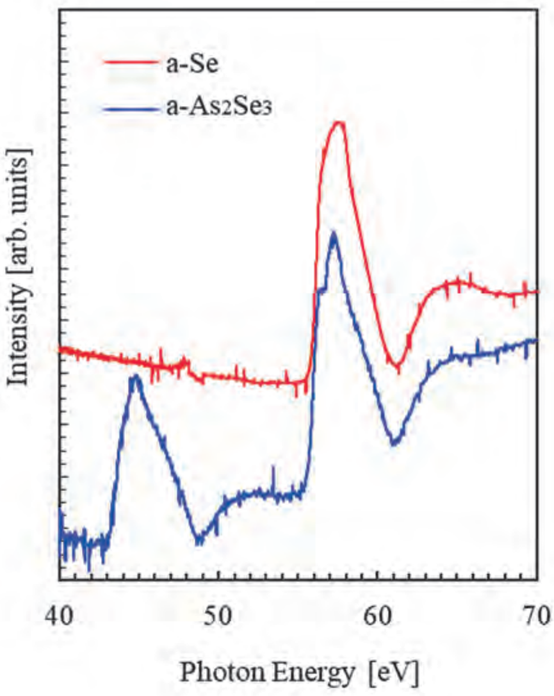

Fig. 1. VUV absorption spectra of as-deposited amorphous Se and As_2Se_3 thin films at room temperature.

[1] K. Tanaka, Rev. Solid State Sci. **4** (1990) 641.
[2] K. Shimakawa, A. Kolobov and S. R. Elliott, Adv. Phys. **44** (1995) 475.
[3] K. Tanaka, Encyclopedia of Nanoscience and Nanotechnology **7** (2004) 629.
[4] J. Bordas, Phil. Mag. **34** (1976) 501.

BL4B

Tuning Surfaces and Interfaces of FeNi Alloy Thin Films by Nitrogen Surfactant Effects

T. Miyamachi[1], K. Kawaguchi[1], Y. Takahashi[1,2], T. Iimori[1], T. Hattori[1], T. Koitaya[3,4],
K. Yamamoto[3,4], M. Kotsugi[2], T. Yokoyama[3,4] and F. Komori[1]
[1]Institute for Solid State Physics (ISSP), The University of Tokyo, Kashiwa 277-8581, Japan
[2]Faculty of Industrial Science and Technology, Tokyo University of Science, Tokyo 125-8588, Japan
[3]Department of Materials Molecular Science, Institute for Molecular Science, Okazaki 444-8585, Japan
[4]Department of Structural Molecular Science, The Graduate University for Advanced Studies, SOKENDAI,
Okazaki 444-8585, Japan

A rare-metal-free ferromagnetic $L1_0$-type FeNi ordered alloy attracts much attention due to its expected strong uniaxial magnetic anisotropy. Previous studies reported the preparation of $L1_0$ FeNi films by several thin film growth techniques such as layer-by layer molecular beam epitaxy (MBE) and pulse laser deposition (PLD). However, the perpendicular magnetic anisotropy of $L1_0$ FeNi has not been achieved so far possibly due to an imperfect layer-by-layer stacking and intermixing at the Fe/Ni interface during growth processes, which results in the low structural ordering.

To realize high-quality FeNi alloy thin films, we incorporate nitrogen surfactant effects of monatomic layer magnetic nitrides into the alternate Fe and Ni deposition. The nitrogen surfactant epitaxy intends to suppress the interdiffusion at the Fe/Ni interface during the deposition and annealing processes and keeps atomically flat surface/interface. The validity of this approach on structural and magnetic properties of FeNi alloy thin films were confirmed for 1 monolayer (ML) Fe on Ni_2N/Cu (001), which is the initial fabrication step, by scanning tunneling microscopy (STM) and x-ray absorption spectroscopy/x-ray magnetic circular dichroism (XAS/XMCD). We observed structural changes of the system from Fe/Ni_2N/Cu(001) to FeN/Ni/Cu(001) induced by the nitrogen surfactant effect while keeping the high quality Fe/Ni interface even after annealing process at 420 K, and resultingly the enhancement of the perpendicular anisotropy [1,2].

In this work, we grow thicker FeNi alloy thin films up to tri- and quadruple-layers (NiN/Fe/Ni and FeN/Ni/Fe/Ni) and investigate the impact of surface/interface modifications with increasing the film thickness on their electronic and magnetic properties by STM and XAS/XMCD [3].

The Ni_2N was grown on Cu(001) by following fabrication processes of a monatomic layer iron nitride (Fe_2N) [4]. The quality of the Ni_2N was prechecked by STM and LEED before XAS/XMCD measurements. Then, 1 ML Fe and Ni were alternatingly deposited at ~ 150 K to grow tri- and quadruple-layers. XAS/XMCD measurements were performed at BL4B in UVSOR by total electron yield mode at B = 0 - ± 5 T and T = 7.9 K. The XMCD spectra are obtained at the normal (NI: $\theta = 0°$) and the grazing (GI: $\theta = 55°$) geometries. Magnetization curves were recorded by plotting the L_3/L_2 XAS intensity as a function of the magnetic field.

We find from the magnetization curve that the magnetization easy axis of the trilayer is toward the out-of-plane direction. This indicates that the out-of-plane magnetocrystalline anisotropy of the trilayer is large enough for overcoming the in-plane film shape anisotropy. On the other hand, the quadruple layer shows the strong in-plane magnetic anisotropy. The results could be interpreted from the modification of the topmost surface layer from NiN (trilayer) to FeN (quadruple layer), which presumably prefers the in-plane magnetization [5].

[1] T. Miyamachi *et al.*, UVSOR Activity Report 2018 **46** (2019) 138.
[2] T. Miyamachi *et al.*, UVSOR Activity Report 2018 **46** (2019) 139.
[3] K. Kawaguchi *et al.*, Phys. Rev. Materials *accepted.*
[4] Y. Takahashi *et al.*, Phys. Rev. Lett. **116** (2016) 056802.
[5]Y. Takahashi *et al.*, Phys. Rev. B **95** (2017) 224417.

BL4B

Magnetic Properties of FeCo Alloy Thin Films Grown by Nitrogen Surfactant Epitaxy

T. Miyamachi[1,2], Y. Takahashi[1,3], T. Hattori[1], T. Koitaya[4,5], K. Yamamoto[4,5], M. Kotsugi[3],
T. Yokoyama[4,5] and F. Komori[1]
[1]*Institute for Solid State Physics, The University of Tokyo, Kashiwa277-8581, Japan*
[2]*The University of Electro- Communications, Chofu 182-8585, Japan*
[3]*Tokyo University of Science, Tokyo 125-8588, Japan*
[4]*Institute for Molecular Science, Okazaki 444-8585, Japan*
[5]*The Graduate University for Advanced Studies, SOKENDAI, Okazaki 444-8585, Japan*

An $L1_0$-type FeCo ordered alloy is theoretically predicted to show an extraordinary large perpendicular magnetic anisotropy among transition metal alloys, attracting great attention as a rare earth-free permanent magnet. The precisely controlled thin film growth of alternating Fe and Co atomic layers using pulsed laser deposition have been used for the preparation of $L1_0$ FeCo thin films [1]. However, the degree of order of the $L1_0$ structure is still low due to atomic-scale structural and magnetic disorder at the Fe/Co interface and resultingly the perpendicular magnetization has not yet been achieved.

Toward realizing high quality FeCo alloy thin films, we here focus on the fabrication method utilizing nitrogen surfactant effects of monatomic layer iron and cobalt nitrides (Fe_2N and Co_2N). The validity of the nitrogen surface epitaxy on the growth of $L1_0$-type alloy thin films has been demonstrated for FeNi alloy thin films [2]. High lateral lattice stability of magnetic nitrides [3], and the surfactant nitrogen during the deposition of Fe and Co atomic layers can effectively suppress the interdiffusion at the Fe/Co interface, leading to atomically flat and homogeneous surface and interface in FeCo alloy thin films.

We here performed combined study of scanning tunneling microscopy (STM) and x-ray absorption spectroscopy/x-ray magnetic circular dichroism (XAS/XMCD) to investigate structural and magnetic properties of 1 monolayer (ML) Co on Fe_2N/Cu (001), the initial step for the fabrication of FeCo alloy thin films grown by the nitrogen surfactant epitaxy. The advantage of this complementary experimental approach is that macroscopic observations of element specific and quantitative electronic and magnetic properties by XAS/XMCD can be linked with microscopic origins of the Fe/Co interface characteristics revealed by STM [4].

The monatomic layer of Fe_2N was grown on Cu(001) in the following processes: (1) N^+ bombardment onto a clean Cu(001) surface with a beam energy of 500 eV, (2) Fe deposition onto N/Cu(001) at room temperature, and (3) subsequent annealing up to ~ 670 K [3]. 1 ML Co was thereafter deposited at a low temperature (~ 150 K).

XAS/XMCD measurements were performed at BL4B in UVSOR by total electron yield mode at $B = 0 - \pm 5$ T and $T = 6.6$ K. The XMCD spectra are obtained at the normal (NI: $\theta = 0°$) and the grazing (GI: $\theta = 55°$) geometries by detecting $\mu_+ - \mu_-$, where μ_+ (μ_-) denotes the XAS recorded at Fe and Co L adsorption edges with the photon helicity parallel (antiparallel) to the sample magnetization. Note that θ is the angle between the sample normal and the incident x-ray. Magnetization curves were recorded by plotting the L_3 XAS intensity normalized by the L_2 one as a function of the magnetic field.

We first confirmed from XMCD measurements the strong in-plane magnetic anisotropy of bare Fe_2N as previously reported [3]. STM measurements revealed the formation of Co_2N/Fe/Cu (001) via nitrogen surfactant effect by adding 1 ML Co. Accordingly, relative increase in the out-of-plane magnetization of Fe to the in-plane magnetization was observed. These results indicate that the nitrogen surfactant effect efficiently suppresses the interdiffusion at the Fe/Co interface and keeps atomically flat surface/interface in FeCo atomic layers, presumably reflecting the intrinsic out-of-plane magnetization of $L1_0$ FeCo.

[1] H. Ito *et al.*, AIP Advances **9** (2019) 045307.
[2] K. Kawaguchi *et al.*, Phys. Rev. Materials, *accepted*.
[3]Y. Takahashi *et al.*, Phys. Rev. B **95** (2017) 224417.
[4] S. Nakashima *et al.*, Adv. Funct. Mater. **29** (2019) 1804594.

BL4B

Molecular Orientation and Magnetic Properties of Iron Phthalocyanine Thin Films Grown on Passivated Silicon Surfaces

S. Ohno[1], K. Yamamoto[2], T. Koitaya[2] and T. Yokoyama[2]
[1]*Fuclty of Engineering, Yokohama National University, Yokohama 240-8501, Japan*
[2]*Institute for Molecular Science, Okazaki 444-8585, Japan*

Iron phthalocyanine (FePc) is one of the prototype molecules to study magnetic properties of molecular thin films. It is a planner molecule which has an Fe^{2+} iron at the center. It has been shown that the first Hund's rule is violated in FePc, resulting in the ground state of S=1 rather than S=2 [1]. It has been reported that highly unquenched orbital moment is caused by the ^3E_g ground state with the half-filled e_g state at the Fermi level for FePc thin films grown on gold surfaces [2].

In the present work, we studied both molecular orientation and magnetic properties of FePc thin films grown on passivated silicon surfaces, such as water-adsorbed Si(001) (H_2O/Si(001)), oxidized Si(001) (SiO_2/Si(001)) and oxidized silicon wafer covered with monolayer graphene (Gr/SiO_2).

BL4B soft X-ray beamline was used for X-ray Absorption Near Edge Structure (XANES) spectroscopy measurements in N K-edge region and X-ray Magnetic Circular Dichroism (XMCD) measurements in Fe L-edge region.

Figure 1 shows angle-dependent linearly polarized XANES spectra at the N K-edge. The peaks A, B, and C are assigned to π* resonances and D, E, and F are assigned to σ* resonances [2]. In the present cases, the tilted angles of the molecular plane are estimated to be ~35-65° on average. These suggest that the FePc molecules are not perfectly aligned parallel to the surface nor perpendicular to the surface.

Figure 2 shows MCD spectra of FePc/Gr/SiO_2 at the Fe L-edge. We have evaluated the orbital magnetic moment (m_L) and the spin magnetic moment (m_S) using the sum rules. The values of m_L are estimated to be ~0.1-0.8 μ_B, depending on the thickness and substrate. In several cases, the values are even larger than the reported values (~0.2-0.5 μ_B) obtained for FePc/Au [2].

The present results indicate that the properties of FePc thin films grown on H_2O/Si(001) and SiO_2/Si(001) are similar in the molecular orientation as well as the magnetic moment. In contrast, the MCD spectra exhibit quite different features in the case of FePc thin films grown on Gr/SiO_2. For instance, the two distinct peaks are observed in the L_{III} region, as shown in Fig. 2. These may correspond to the a_{1g} and e_g states observed for the well-ordered films [2]. The role of monolayer graphene is found to be substantial to modify both molecular orientation and magnetic properties.

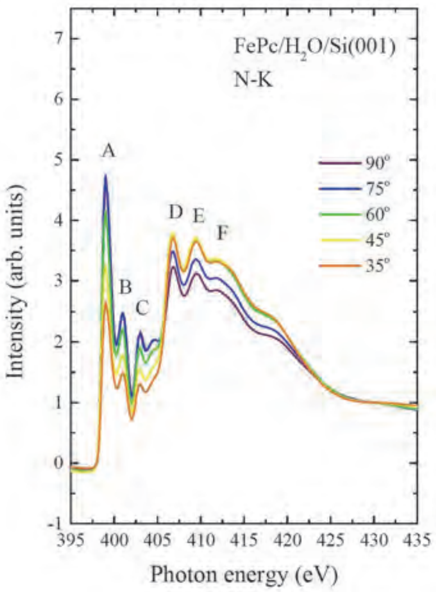

Fig. 1. Angle-dependent linearly polarized XANES spectra of FePc/H_2O/Si(001) at the N K-edge.

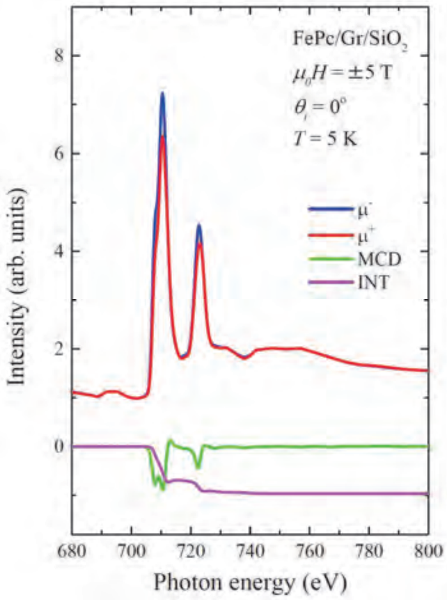

Fig. 2. MCD spectra of FePc/Gr/SiO_2 at the Fe L-edge.

[1] M.D. Kuz'min *et al.*, Phys. Rev. B **79** (2009) 024413.
[2] J. Bartolomé *et al.*, Phys. Rev. B **81** (2010) 195405.

BL5U

Polarization Dependent Interfacial Electronic Structure of Ultra-thin Fe Layers on Rashba-splitted Au (111) Surfaces

J. Okabayashi[1], K. Tanaka[2] and S. Mitani[3]

[1]*Research Center for Spectrochemistry, The University of Tokyo, Tokyo 113-0033, Japan*
[2]*UVSOR Synchrotron Facility, Institute for Molecular Science, Okazaki 444-8585, Japan*
[3]*National Institute for Materials Science, Tsukuba 305-0047, Japan*

When ferromagnetic transition metals (TMs) are deposited on the Rashba-type spin-orbit coupled surface, novel properties such as perpendicular magnetic anisotropy (PMA) are emerged at the interfaces, which are derived from the symmetry broken spin-orbit effects. The gold Au (111) surfaces have been investigated extensively by means of scanning tunneling microscopy and angle-resolved photoemission spectroscopy (ARPES) because this surface exhibits the large Rashba-type spin-orbit splitting of 110 meV [1]. It provides the wide varieties for the topological physics and spin-orbit coupled sciences at the surfaces and interfaces. Recently, the interfaces between Au(111) and other heavy elements such as Bi or Ag have been extensively investigated [2,3]. Here, we focus on the interfaces between ferromagnetic materials and Au(111) interfaces because the thin Fe layers on the heavy elements are expected to exhibit the PMA induced by the Rashba-type spin-orbit interaction.

The spin-orbit coupling between the ferromagnetic 3*d* TMs Fe or Co and 5*d*, 6*sp* heavy metal elements of non-ferromagnetic materials such as Pt and Au has been utilized for the PMA through the proximity at the interfaces. It is believed that the future researches concerning not only spins but also orbitals are recognized as the *spin-orbitornics*. Therefore, to clarify the origin of the PMA at these interfaces is a crucial role. The relationship between Au (111) Rashba-type spin-orbit interaction and PMA in 3*d* TMs has not been clarified explicitly. In order to investigate the orbital-resolved states in the Fe films showing the PMA, ARPES at the interfaces becomes powerful techniques through the photon-energy and polarization dependences in each 3*d* orbital. By using ARPES, we aim to understand the orbital-resolved electronic structures at the magnetic interfaces on the Rashba-type Au (111) surface in order to develop the researches of novel PMA using spin-orbit coupled interfaces.

We prepared the clean Au (111) surface for the Fe deposition. The commercialized single-crystalline 100-nm-thick Au (111) films on sapphire substrate were used. At the beamline BL5U in UVSOR, we repeated the Ar-ion sputtering at 1 kV accelerating voltage and subsequent annealing at 400 °C under the high vacuum conditions. After the sample preparation, the Fe layer was deposited at room temperature and then annealed. By *in-situ* transferring the samples into the ARPES chamber, we performed ARPES at 10 K using the photon energies of 60 and 120 eV because of the large cross-section of Au (111) surface states and detections of Fe 3*s* and Au 4*f* intensity ratios, respectively.

Figures 1 (a) and (b) display the photoemission spectra in Fe layers on Au (111) with horizontally and vertically polarized beams at 60 eV. As shown in Fig. 1a, the intensity ratio changes due to the difference of orbital symmetry. The Au (111) surface clearly exhibits the Rashba-type surface states. The Fe 3*d* states appear near the Fermi level (E_F) and the surface states disappear. As shown in Fig. 1 (c), band dispersion image plots taken by horizontal and vertical polarized beams exhibit asymmetric feature, which can be explained by the Fe 3*d* orbital-resolved states through the overlap between Fe and Au. Horizontal and vertical cases detect preferentially out-of-plane and in-plane orbitals, respectively. Furthermore, we confirmed the PMA at Fe/Au interface by x-ray magnetic circular dichroism and Mössbauer spectroscopies. Therefore, the interfacial chemical reaction between Fe and Au brings the novel properties on the ultrathin Fe electronic structures.

We acknowledge Dr. S. Ideta in IMS for technical supports of data analyses. This work was in part supported by KAKENHI Kiban(S) project.

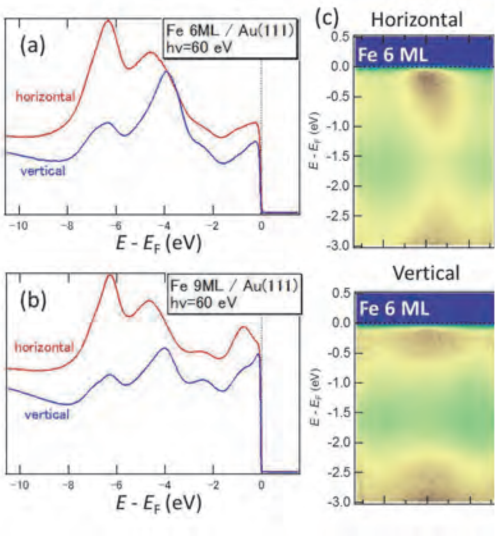

Fig. 1. Polarization dependence in Fe valence-band photoemission spectra taken at 60 eV for (a) 6 ML and (b) 9 ML. (c) Band-dispersion mapping of Fe 6 ML case for horizontal and vertical beams taken at 60 eV.

[1] S. LaShell *et al.*, Phys. Rev. Lett. **77** (1996) 3419.
[2] C. Tusche *et al.*, Ultramicroscopy **159** (2015) 620.
[3] B. Yan *et al.*, Nature Commun. **6** (2015) 10167.

BL5U

Electronic Structure of Ultrathin Bismuth Films Fabricated on InSb(111)

Y. Ohtsubo[1,2], J. K. Modak[2], T. Nakamura[2] and S. Kimura[1,2]
[1]*Gradudate School of Frontier Biosciences, Osaka University, Suita 565-0871, Japan*
[2]*Department of Physics, Graduate School of Science, Osaka University, Toyonaka 560-0043, Japan*

The electronic structure of elemental bismuth (Bi) has been studied extensively in this decade because of its ambiguous three-dimensional topological order driven by the large size of spin-orbit interaction in valence bands [1]. Moreover, ultrathin Bi film down to few monatomic layers is also predicted as a two-dimensional topological insulator [2] and hence is gathering much attention. Although growth of Bi ultrathin films with several layers has been achieved on various substrates [3-5], most of them are strongly influenced from substrates, such as the significant structural deformation on SiC [3] and intermixing with the metallic states of the Bi_2Te_3 substrate [4]. In this project, we tried to grow ultrathin Bi films with a few layers on InSb(111), which has the lattice constant very close to the Bi crystal and no electronic states around the Fermi level. These characteristics of InSb suggest that it is a suitable substrate to realize free-standing Bi ultrathin films down to 1-2 bilayers (BL).

The InSb(111) substrates were cleaned in an ultra-high vacuum chamber by repeated cycles of Ar ion sputtering with the ion energy of 1 keV and annealing with the temperature of 550 K until a sharp RHEED pattern was observed. Subsequent evaporation of Bi was performed on the substrate at room temperature using a home-made Knudsen cell, resulting in sharp and low-background patterns as shown in Fig. 1 (a). It suggests that high-quality Bi(111) films were obtained by this method. The Bi evaporation rate was checked *in-situ* by monitoring the intensity oscillation of the RHEED diffraction rods. Accordingly, we could fabricate the ultrathin Bi(111) films with the thicknesses from 1 to 5 BLs. The film thicknesses were cross-checked by core-level photoelectron peak areas of Bi, In, and Sb, showing a consistent behavior to the RHEED oscillation.

Figure 1 (b) shows the Fermi contour of the 5-BL Bi(111) film grown on InSb(111) obtained by ARPES. The six-fold tear-drop like contours and nearly circular one at the center of the surface Brillouin zone are consistent with the earlier results [1,5]: the latter should be hexagonal, but it is difficult to distinguish hexagon and circle with the current angular resolution. This agreement suggests that the obtained Bi(111) film, especially its electronic structure around the Fermi level, is free from any modulations by substrates. At the lower thicknesses, the shape of the Fermi contour as well as the surface-band dispersions changed according to the thicknesses. Detailed analysis of such changes, especially a comparison with theoretical calculations are ongoing in order to examine whether the fabrication of the free-standing Bi(111) films with 1-2 BLs, a promising playground to study the topological edge states of two-dimensional topological insulators, could be achieved or not.

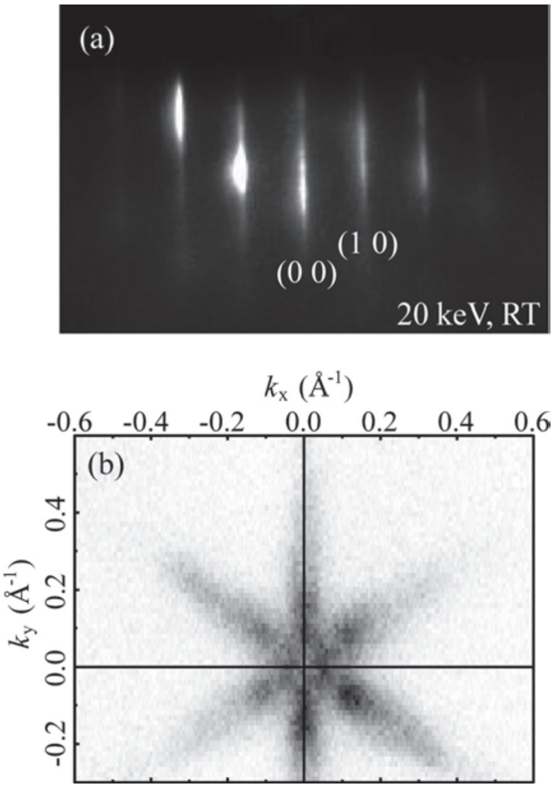

Fig. 1. (a) RHEED pattern of the Bi(111) film (5 BL) on InSb(111). (b) Fermi contour of the same sample taken by ARPES (*hν*= 60 eV, 7 K).

[1] L. Fu and C. L. Kane, Phys. Rev. B **76** (2007) 045302. S. Ito *et al.*, Phys. Rev. Lett. **117** (2016) 236402. Y. Ohtsubo and S. Kimura, New J. Phys. **18** (2016) 123015 and references therein.
[2] S. Murakami, Phys. Rev. Lett. **97** (2006) 236805.
[3] F. Reis *et al.*, Science **357** (2017) 287.
[4] T. Hirahara *et al.*, Phys. Rev. Lett. **107** (2011) 166801.
[5]T. Hirahara *et al.*, Phys. Rev. Lett. **97** (2006) 146803.

BL5U, BL7U

Thermal Effect of the Surface Reconstruction of the Topological Kondo Insulator SmB_6

Y. Ohtsubo[1,2], T. Nakamura[2], T. Nakaya[2], F. Iga[3] and S. Kimura[1,2]
[1]*Graduate School of Frontier Biosciences, Osaka University, Suita 565-0871, Japan*
[2]*Department of Physics, Graduate School of Science, Osaka University, Toyonaka 560-0043, Japan*
[3]*College of Science, Ibaraki University, Mito 310-8512, Japan*

Topological Kondo Insulators (TKI) are gathering much attention in these days as an interesting playground to study the concert effect of the spin-polarized topological surface states and strong electron correlation resulting in the metal-insulator transition of Kondo insulators [1]. Samarium hexaboride (SmB_6) is the first and the most extensively studied candidate of TKI. It has been revealed that the (001) surface of a cleaved SmB_6 single crystal hosts the metallic and spin-polarized surface states as expected from topological classification [1,2]. However, the topological order of SmB_6 itself is still under debate because of the multiple possible interpretations of the metallic surface bands [3,4] as well as the various surface atomic structures randomly appear on the cleaved surfaces [5].

In this project, we have revisited the surface atomic and electronic structures of SmB_6(001) by using the *in-situ* cleaning method in an ultra-high vacuum (UHV) chamber. The (001) faces of SmB_6 single crystals were polished under air atmosphere and then cleaned in the UHV chamber by repeated cycles of Ar^+ sputtering (ion energy: 1 keV) and annealing. The annealing temperature was set at several temperatures from 600 to 1400 °C and the surface atomic and electronic structures were checked at each temperature by LEED and ARPES measurements, respectively.

As shown in Fig. 1 (a), we found the (2×1) surface reconstruction with the annealing temperature of 800 °C. The fractional order spots became weak and diffused with the elevated annealing temperature up to 1000 °C. Afterward, at the highest annealing temperature (1400 °C), the fractional-order spots appeared again with the sharper shape than those after 800 °C annealing, (see Fig. 1 (b)). These (2×1) surface reconstructions are consistent with the known surface structures [3,5-7].

Figure 1 (c) shows the B-1*s* core-level photoelectron spectra corresponding to the LEED patterns shown in Figs. 1 (a, b). At 800 °C (the lower spectrum), a satellite peak around 16.7 eV is shown, suggesting the surface reconstruction by boron, which would originate from displacements of B_6 clusters. In contrast, at 1400 °C (the upper), no such satellite observed in the spectrum. It suggests that the latter (2×1) surface reconstruction does not originate from the surface boron but from the other reasons such as periodic desorption of Sm atoms from the surface atomic layers.

These two different (2×1) surfaces on SmB_6(001) could reconcile the wide variety of surface preparation conditions reported so far [6,7]. Further analysis on the surface electronic structure around the Fermi level, especially the influence from the newly distinguished surface reconstructions, is ongoing.

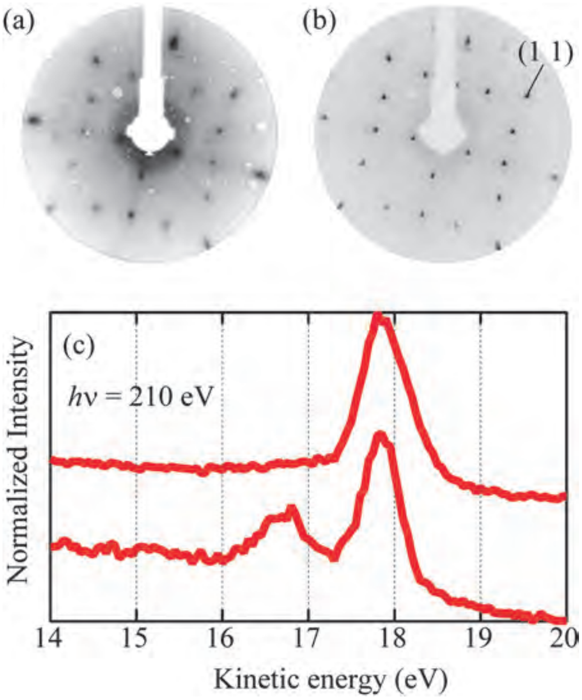

Fig. 1. (a, b) LEED patterns (The pass energy: $E_P = 44$ eV) of the SmB_6(001)-(2×1) surfaces annealed at (a) 800 °C and (b) 1400 °C. (c) B-1*s* core-level spectra taken from the SmB_6(001)-(2×1) surfaces; the lower (upper) one is from the surface annealed at 800 (1400) °C.

[1] M. Dzero *et al.*, Phys. Rev. Lett. **104** (2010) 106408.
[2] N. Xu *et al.*, J. Phys.: Condens. Matt. **28** (2016) 363001 and references therein.
[3] P. Hlawenka *et al.*, Nat. Commun. **9** (2018) 517.
[4] Y. Ohtsubo *et al.*, Nat. Commun. **10** (2019) 2298.
[5] S. Rößler *et al.*, PNAS **111** (2014) 4798.
[6] H. Miyazaki *et al.*, Phys. Rev. B **86** (2012) 075105.
[7] M. Ellguth *et al.*, Philos. Mag. **96** (2016) 3284.

BL6U

Photoemission Tomography Utilizing One-dimensionally Ordered Film of High-mobility Organic Semiconductors

M. Iwasawa[1], S. Kobayashi[1], Y. Hasegawa[2], M. Nozaki[3], S. Kurihara[3], S. Otaki[3], K. Niki[3], M. Sasaki[1], F. Matsui[2], S. Kera[2] and Y. Yamada[1]
[1]*Institute of Applied Physics, University of Tsukuba, Tsukuba 305-8573, Japan*
[2]*Institute for Molecular Science, Department of Photo-Molecular Science, Okazaki 444-8585, Japan*
[3]*Institute of Applied Physics, Chiba University, Tsukuba 305-8573, Japan*

Recently, the researches of the photoelectron tomography (PT) of the organic semiconductor films have rapidly been increased with many successes to obtain the information of the character of the initial-state wavefunction. However, the researches have still been limited to the model molecules with simple molecular shape. In this work, we tried to apply PT to rather practical organic semiconductor molecules with high mobility, in order to clarify the mechanism of their charier transport.

In the present study, we especially focused on the practical molecules with rather simple structure, such as picene and Dph-BTBT. The single crystals and films of these molecules are known to show lather high mobility up to the range of 10^1 cm^2/Vs. Recent theoretical calculation have shown that, while the hole mobility in the case of picene can be rather fairly explained considering the HOMO, that in the case of BTBT cannot be understood only by HOMO. In the case of BTBT, HOMO-1 must be taken into account, despite the energy difference between HOMO and HOMO-1 of BTBT is much larger than that of picene. The PT analysis can shied the light on the nature of the molecular orbital which is responsible in the carrier transport.

We utilized well-defined thin film of picene and Dph-BTBT film utilizing anisotropic Ag(110) substrate. The molecular arrangements in these films were directly determined LEED and STM. PT of these system were done at BL6U of UVSOR. In the PT measurements, we utilized mesh electrode in front of the sample which was at +500 V with respect to the sample, in order to increase the acceptance angle of the photoelectron to probe wider area in the reciprocal space.

Figure 1 (a) shows the one-dimensional structure of the picene films on Ag(110) substrate, where the molecular axis of picene is aligned [1-10] direction of the substrate. Figure 1 (b) is corresponding photoelectron angular distribution (PAD) mapping patterns for HOMO and HOMO-1. The obtained patterns well correspond to the Fourier transform (FT) of the each molecular orbitals as shown in the inset. We then extract the energy distribution curve (EDC) from the portion of the rectangles in the PAD mapping, as shown in Fig. 1 (c) Although the area averaged EDC showed overlapped spectrum, selected-area accumulation clearly shows the EDC of HOMO and HOMO-1.

Figure 2 shows the results of Dph-BTBT. In contrast to the case of picene, the molecular long axis of Dph-BTBT/Ag(110) was not in the [1-10] direction and two different domains were found. In this case, the energy of the HOMO and HOMO-1 levels are well separated and their PAD are rather similar, in contrast to the case of picene. However, we can clearly separate the photoelectrons from these levels in PAD mapping, which will be useful in the discussion of the overlapping of these orbitals.

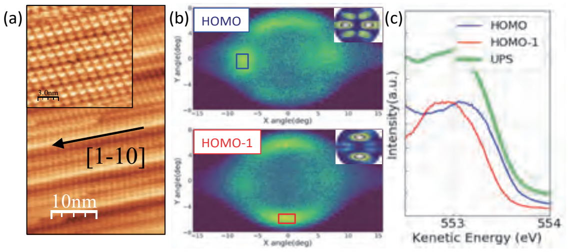

Fig. 1 (a) STM image of several layer of Picene/Ag (110). (b) PAD images of HOMO and HOMO-1 (c) selectred-area EDC of HOMO and HOMO-1.

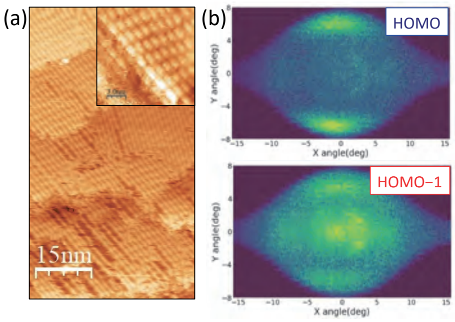

Fig. 2 (a) STM image of monolayer of Dph-BTBT/Ag (110). (b) PAD images of HOMO and HOMO-1.

BL6U

ARPES and RAES Study of Nanographene on Pt(111)

O. Endo[1,3], F. Matsui[2], W.-J. Chun[3], M. Nakamura[4], K. Amemiya[5] and H. Ozaki[1]
[1]Department of Applied Chemistry, Faculty of Engineering, Tokyo University of Agriculture and Technology, Koganei 184-8588, Japan
[2]UVSOR Synchrotron Facility, Institute for Molecular Science, Okazaki 444-8585, Japan
[3]Graduate School of Arts and Sciences, International Christian University, Mitaka 181-8585, Japan
[4]Department of Applied Chemistry and Biotechnology, Faculty of Engineering, Chiba University, Chiba 263-8522, Japan
[5]Photon Factory, High Energy Accelerator Research Organization (KEK-PF), Institute of Materials Structure Science (IMSS), Tsukuba 305-0801, Japan

Graphene, a single sheet of carbon, is one of typical 2D materials which exhibits a peculiar band structure. Nanographene (NG), which is cut from graphene into nano-size, is expected as a material for next generation devices due to the confined electronic structure and an open band gap. In this study, Angular Resolved Photo Emission Spectroscopy (ARPES) and Resonant Auger Electron Spectroscopy (RAES) were performed to investigate the electronic structure of NG.

NG was obtained by the thermal decomposition of benzene on the Pt(111) surface at the substrate temperature of either 1100 K (HT) or 800 K (LT). All the spectra were measured at BL6U of UVSOR.

Figure 1 shows the band dispersion along the Γ-K direction of the NGs on Pt(111). Both the NGs obtained at HT(a) and LT(b) exhibit the π band, and therefore, the π band is formed for the NG obtained at LT with the size of as small as 10 nm diameter, which was confirmed by scanning tunneling microscopy. The size of NG obtained at HT is estimated > 100 nm diameter. The NG lattice is rotated ca. 30° with respect to the Pt lattice. The bottom of the π band is located at 7.8 eV from E_F, which is shallower than that of graphite (8.16 eV) [1]. This indicates the electron transfer to the Pt substrate [2,3]. Figures 2 (a) and (b) show the C1s XPS spectra. In addition to the principal peaks at BE = 283.9 eV (sp2 carbon of graphene), a shoulder at 284.2 eV is enhanced for the NG obtained at LT. This shoulder suggests the existence of the sp3 carbon, which forms the C-Pt bond [4]. This is consistent with the Pt4f XPS spectra shown in Figs. 2(c) and (d), which exhibit a smaller surface-related band at 70.7 eV for the NG obtained at LT. Figure 3 shows the RAE spectra excited at the photon energy of $1s \rightarrow \pi^*$ transition. Although the angular dispersion is observed for the NG obtained at HT, which is similar to graphite [5], the auger electrons are focused at the Γ point for the NG obtained at LT. Similar dispersion patterns are observed for all the excitation energies in the C K-edge region.

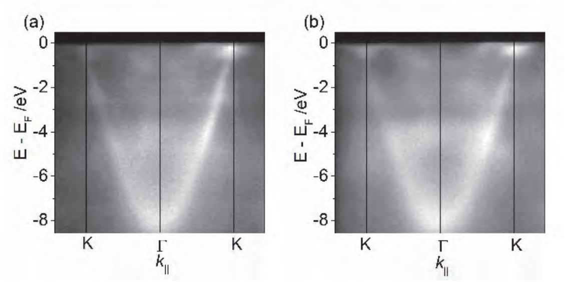

Fig. 1. π band of NG obtained at (a)HT and (b)LT.

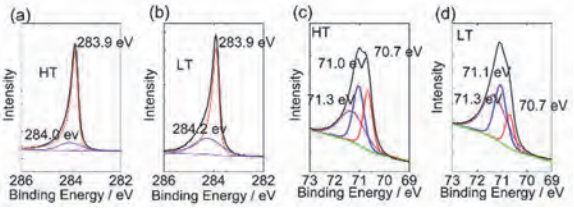

Fig. 2. C1s XPS of NG obtained at (a)HT and (b)LT. Pt 4f XPS of NG obtained at (c)HT and (d)LT.

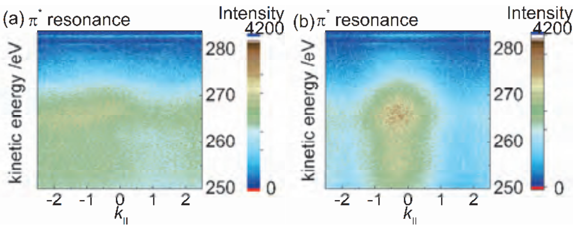

Fig. 3. RAES at C K-edge of NG obtained at (a)HT and(b)LT.

[1] F. Matsui *et al*., Phys. Rev. B **97** (2018) 045430.
[2] G. Giovannetti *et al*., Phys. Rev. Lett. **101** (2008) 026803.
[3] P. Sutter *et al*., Phys. Rev. B **80** (2009) 245411.
[4] S. Rajasekaran *et al*., Phys. Rev. B **86** (2012) 075417.
[5] F. Matsui *et al*., JPS 2019 Autumn meeting.

BL7U

High-resolution Angle-resolved Photoemission Study on $MnBi_2Te_4/Bi_2Te_3$

S. Kusaka[1], K. Sumida[1], T. Fukasawa[1], S. Ichinokura[1], S. Ideta[2], K. Tanaka[2] and T. Hirahara[1]
[1]*Department of Physics, Tokyo Institute of Technology, Tokyo 152-8551, Japan*
[2]*UVSOR Synchrotron Facility, Institute for Molecular Science, Okazaki 444-8585, Japan*

Topological insulators (TI) are extensively studied recently due to its peculiar properties [1]. The Dirac-cone surface states of TI are protected by time-reversal symmetry (TRS) and backscattering among these surface states is prohibited. But when TRS is broken by application of a magnetic field or incorporating magnetic materials, a gap opening in the Dirac cone is expected and an intriguing phase called the quantum anomalous Hall state can be realized [2]. This phase is expected to show even more exotic phenomena such as the topological magnetoelectic effect. To realize such state, two types of sample fabrication techniques have been employed up to now: (1) magnetic doping while growing the single crystal or thin film of TI [3], and (2) magnetic impurity deposition on the surface of TI [4]. While method (1) was successful and showed evidence of the TRS violation, no one has succeeded using method (2), which should be a more direct way to examine the interaction between the topological surface states and magnetism. We have previously found another novel technique to induce magnetism into TI, namely the magnetic extension effect [5]. By depositing Mn and Se on Bi_2Se_3, we found that Mn and Se are incorporated in the topmost Bi_2Se_3 layer and a novel heterostructure $MnBi_2Se_4/Bi_2Se_3$ is formed [5]. This heterostructure showed a clear Dirac cone gap of 85 meV and the gap persisted up to room temperature. From magnetic measurements it was revealed that ferromagnetism also persists up to room temperature in this system. Taking all these facts into account, it can be said that this system is promising to observe the quantum anomalous Hall effect at room temperature. However, the Dirac cone gap is not at the Fermi level and there is no systematic method to control the Fermi level position in Bi_2Se_3.

Therefore in this study, we have employed Bi_2Te_3 as the parent TI and have deposited Mn and Te on Bi_2Te_3 to see if magnetic extension can also occur for this system. Our structural analysis based on LEED-IV measurements ensured that the heterostructure we fabricated was $MnBi_2Te_4/Bi_2Te_3$. The band dispersion measured at 10 K is shown in Fig. 1. In contrast to the $MnBi_2Se_4/Bi_2Se_3$ sample, there was no gap opening in the surface Dirac cone of $MnBi_2Te_4/Bi_2Te_3$ even at 10 K. We have also performed X-ray magnetic circular dichroism measurements on this heterostructure and found that it is paramagnetic down to 5.6 K, the lowest temperature we can reach in the experimental system. Thus the absence of the Dirac cone gap and its correspondence with the magnetic properties is clear-cut in this system. The remaining questions are: (1) why is this structure paramagnetic down to 5.6 K in contrast to the theoretical calculations that predict a Curie temperature of 12 K [6] with a 77 meV Dirac cone gap [7]? (2) why is the magnetic property of this system so different from that of $MnBi_2Se_4/Bi_2Se_3$? We hope to resolve these questions in the near future from further investigation.

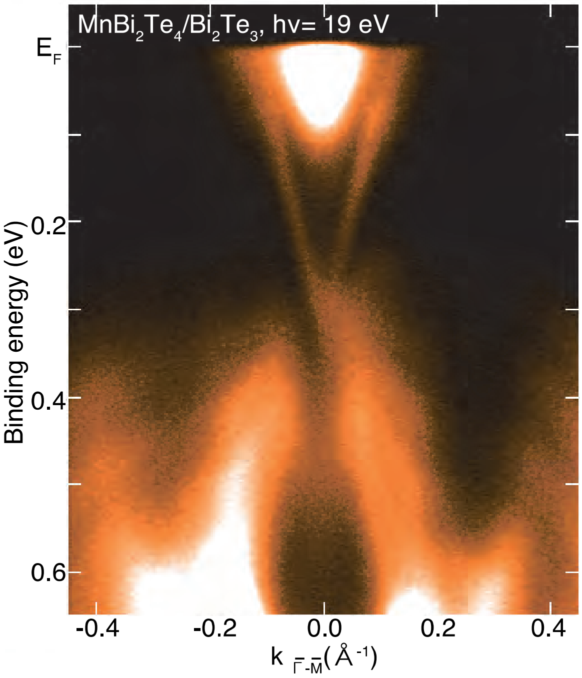

Fig. 1. Band dispersion image of the $MnBi_2Te_4/Bi_2Te_3$ heterostructure measured at 10 K.

[1] M. Hasan and C. Kane, Rev. Mod. Phys. **82** (2010) 3045.
[2] X.-L. Qi and S.-C. Zhang, Rev. Mod. Phys. **83** (2011) 1057.
[3] For example, C. Z. Chang *et al.,* Science **340** (2013) 167.
[4] For example, M. Ye *et al.,* Phys. Rev. B **85** (2012) 205317.
[5] T. Hirahara *et al.,* Nano Lett. **17** (2017) 3493.
[6] M. Otrokov *et al.,* Phys. Rev. Lett. **122** (2019) 107202.
[7] M. Otrokov *et al.,* 2D Materials **4** (2017) 025082.

BL7U

Evolution of Electronic Structure of Pentacene Monolayer on Graphite Probed by Low-Energy ARUPS

Y. Hasegawa[1], T. Nakamura[2], M. Meissner[1], T. Yamaguchi[1], S. Ideta[1], K. Tanaka[1] and S. Kera[1]
[1]*Department of Photo-Molecular Science, Institute for Molecular Science, Okazaki 444-8585, Japan*
[2]*Department of Physics, Graduate School of Science, Osaka University, Toyonaka 560-0043, Japan*

Thin films of small organic semiconductor molecules on layered substrates have been widely studied to explore new electronic property and application. The electronic state of the organic thin film can be modified by the subtle change of intermolecular and molecule-substrate interaction which is dominated by weak van der Waals forces. Although impacts of such weak interaction on the electronic state are important to study the mechanism, it has been hardly investigated due to complex and inhomogeneous organic molecular structure.

We have revealed the precise growth of well-ordered thin film of small organic semiconductor molecules on the graphite substrate and investigated the system by means of angle-resolved ultraviolet photoelectron spectroscopy (ARPES) using low-photon energy (hv) excitation (LE-ARUPS). Utilizing the system, we have found modification of the wavefunction despite the weak interaction between the molecule and the substrate [1]. Here, the impact of the structural transition of two-dimensional molecular arrangement in the monolayer of the pentacene/graphite on the electronic structure is investigated by changing the sample temperature. The sample was prepared in a custom UHV chamber. A single crystal graphite (SCG) substrate was cleaned by annealing at 900 K for several hours. Pentacene film of 3 Å was deposited onto the substrate at room temperature. Low-energy electron diffraction (LEED) measurement was performed separately as independent experiments.

First, the structural transition of pentacene monolayer was investigated by taking LEED pattern as shown in Fig. 1. Transition of the LEED pattern from sharp spot to filled hexagon-like pattern with increasing the temperature indicates that the pentacene monolayer with densely packed molecule is formed below the transition temperature (135 K), whereas the monolayer consisting both of molecules which is aligned with a mean distance from adjacent molecules and densely packed molecules with relatively small grains are formed above the transition temperature.

Energy and momentum (E-k) maps of both phases observed by LE-ARPES are shown in Fig. 2. In the E-k maps, flat bands originated from highest occupied molecular orbital (HOMO) of pentacene, consisting of a main peak (00) with the vibrational progressing of satellite peaks toward higher binding energy, (01) and (02), is observed as in the previous works [2]. Below the transition temperature, in addition to the energy shift toward higher energy side, dispersed band at around Γ-point marked by dashed line which is not deribed from a clean graphite is observed (Fig. 2 (a)). This feature is detected only in a certain hv energy region from 7.4 eV to 7.8 eV [1] and shifts with increasing the kinetic energy, indicating that it is possibly originated from resonant excitation of an unoccupied band newly formed for the pentacene molecule and the SCG substrate. This band disappears above the transition temperature, indicating that the electronic state is sensitive to the interfacial structure. These observations suggest that the electronic wave function of pentacene monolayer is connected to that of graphite coherently which causes strong modification of their unoccupied state. The method realizes that the possibility to probe a tailoring of electronic state via weak interaction.

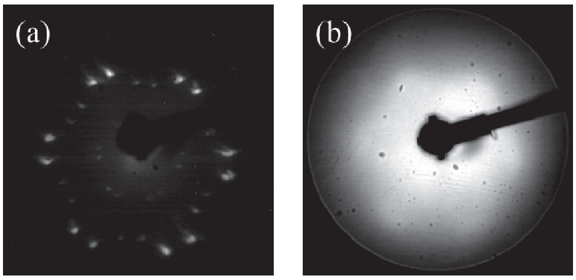

Fig. 1. LEED pattern of pentacene/SCG taken at (a) 72 K and (b) 170 K with electron beam energy of 18 eV.

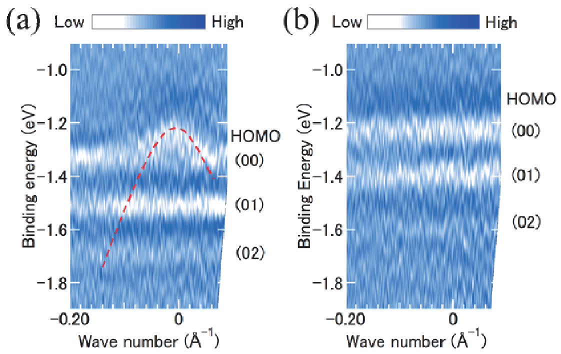

Fig. 2. Second derivative of E-k map taken from pentacene/SCG at (a) 85 K and (b) 165 K with hv = 7.4 eV.

[1] T. Yamaguchi *et al.*, UVSOR Activity Report 2018 **46** (2019) 148.
[2] H. Yamane *et. al.*, Phys. Rev. B **72** (2005) 153412.